Uplink Capacity Optimization for High Throughput Satellites using SDN and Multi-Orbital Dual Connectivity

Michael N. Dazhi, Hayder Al-Hraishawi, Bhavani Shankar Mysore R and Symeon Chatzinotas
Interdisciplinary Centre for Security, Reliability and Trust (SnT), University of Luxembourg.
emails: {michael.dazhi, hayder.al-hraishawi, bhavani.shankar, symeon.chatzinotas}@uni.lu

***Abstract*—Dual Connectivity is a key approach to achieving optimization of throughput and latency in heterogeneous networks. Originally a technique introduced by the 3rd Generation Partnership Project (3GPP) for terrestrial communications, it is not been widely explored in satellite systems. In this paper, Dual Connectivity is implemented in a multi-orbital satellite network, where a network model is developed by employing the diversity gains from Dual Connectivity and Carrier Aggregation for the enhancement of satellite uplink capacity. An introduction of software defined network controller is performed at the network layer coupled with a carefully designed hybrid resource allocation algorithm which is implemented strategically. The algorithm performs optimum dynamic flow control and traffic steering by considering the availability of resources and the channel propagation information of the orbital links to arrive at a resource allocation pattern suitable in enhancing uplink system performance. Simulation results are shown to evaluate the achievable gains in throughput and latency; in addition we provide useful insight in the design of multi-orbital satellite networks with implementable scheduler design.**

I. Introduction

The rapidly growing demand for high data rate and the accentuated resource scarcity in satellite systems require new paradigms to improve radio resource utilization. Of the many candidate techniques, dual connectivity is a promising solution to increase the achievable throughput of the users by utilizing the available resources in heterogeneous systems [1]. Dual connectivity (DC) can increase the per-user data rate without the need for additional bandwidth resources or substantial hardware complexities [2]. DC has been introduced by the 3rd Generation Partnership Project (3GPP) in terrestrial communication networks in Long Term Evolution- (LTE) specification Release 12 in order to enable two radio access networks to simultaneously serve a single user [3]. The technique of dual connectivity has succeeded to boost the performance of terrestrial networks through maximizing the spectrum utilization and satisfying the extremely high throughput requirements in certain circumstances [4].

The capability of satellite systems in providing ubiquitous coverage and extensive access to support various communication applications from diverse industries makes the traffic demands more heterogeneous and geographically distributed. Thus, it is critical for satellite systems to be flexible and adaptive to such spatio-temporal diversified traffic demands [5], and a resilience in allocating the limited satellite resources is essential to satisfy the uneven demands [6]. In this direction, several important contributions to develop flexible resource allocation methods and capacity enhancement approaches have been proposed. For instance, a dynamic capacity allocation scheme is investigated in [7] by utilizing smart gateway diversity structure to minimize system capacity losses and improve rate matching performance. Additionally, the concept of carrier aggregation (CA) for geostationary orbit (GEO) satellites is also studied in [8] but CA has limitations in the multi-orbit satellite structure. Specifically, in CA all component carriers belong to the same system/orbit but in dual connectivity the aggregated carriers can be from different gateways/orbits.

In this context, channel bonding a concept similar to CA was introduced to the satellite systems in the DVB-S2X standard [9]. Apparently, channel bonding standard has some intrinsic limitations that might restrict the required flexibility in resource allocation. For instance, channel bonding is mainly focusing on grouping carriers across transponders, where these carriers have to be intra-band contiguous. Whereas, dual connectivity allows combining multiple carriers from different systems in diverse spectrum bands [10]. Having been motivated by the flexibility offered by dual connectivity beyond the state of the art, this work is considering dual connectivity to circumvent these limitations and improve capacity and flexibility in heterogeneous inter-orbit satellite systems.

Furthermore, the uplink transmission from user equipment towards satellites faces significant challenges than downlink due to the transmit power limitation on the user terminals, which ultimately limits the achievable uplink data rate [11]. In particular, GEO satellites are orbiting constantly at a higher altitude than that of non-geostationary (NGSO) satellites, and thus, GEO uplink losses and latency due to signal propagation are both higher, which is detrimental for delay-sensitive applications. Hence dual connectivity would be useful for satellite operators with multi-orbital constellations such as SES.

Contributions: Our key technical contributions can be explicitly summarized as follows:

1) The design guidelines are stated for deploying a multi-orbital GEO and medium earth orbit (MEO) satellite network with a Hybrid Gateway Station (HGS) serving both GEO and MEO. This includes the introduction of a software defined network controller at the HGS and

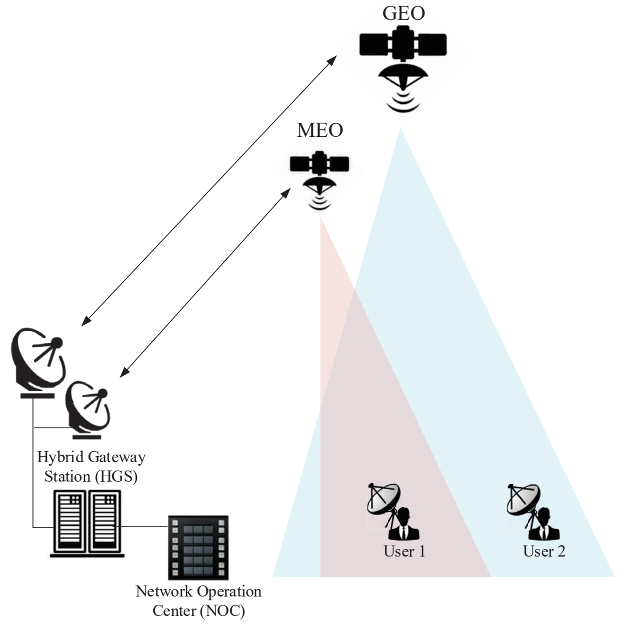

Fig. 1. Schematic diagram of the considered network topology with inter-orbit dual connectivity.

a software defined radio controller at the User Terminal (UT) for the purpose of joint MEO and GEO controlling at the network layer. Focus is placed on MEO for ease of comprehension, this guidelines can be extended to other NGOS like low earth orbit (LEO) constellation.

2) Hybrid resource allocation algorithm has been developed by taking into consideration the satellite channel conditions and the packet arrival rate of the two orbital satellite constellations to achieve an optimal resource allocation pattern, these resources include spectrum and power.
3) The hybrid network performance was evaluated with analyzed link budget results. The proposed hybrid algorithm was also evaluated with simulations in terms of achievable throughput and delay results that were compared with other state-of-the-art algorithms.

The rest of the paper is structured as follows. In section II, the network model and problem analysis are discussed extensively covering system architecture and the proposed hybrid algorithm. Following that in Section III, a performance review of the simulation is given, with the various achievable Key Performance Indicators (KPI). Finally in Section IV, the conclusions are outlined with future work areas summarised.

II. Network Model and Problem Analysis

The objective of this paper is to improve the user experience in a satellite communication system by addressing the problems of delay and capacity. In this context, the paper considers the emerging system with dual connectivity of GEO and MEO, and further aims to offer a network service to minimize latency and maximize throughput.

A. Description of System Architecture

The system architecture consists of a MEO and GEO satellite connected to a HGS that controls and maintains the links. The HGS is configured with two concatenated antennas, each feeding one of the satellites, and the satellites provide beam coverage over the UT. At the HGS, a Gateway Software Defined Network Joint Controller (GSNJC) is configured at the network layer to collect signalling messages on the control plane of both the MEO and GEO links; these messages include packet inter-arrival time, UT DC capability, link signal to noise ratio (SNR), Doppler effect of the satellites and location of the UT. This action is normally handled by a network hub at the gateway, but for the purpose of efficiency and flexibility, Software Defined Network (SDN) controller has been proposed in this architecture to perform these processes. This software controller is a proposed state-of-the-art network control entity for future satellite architecture. Furthermore, GSNJC schedules UT to transmit the packets to the HGS over the MEO and GEO links as shown in Fig. 2.

From the uplink transmitting UT, the Protocol Data Units (PDU) are generated and prepared for transmission at the network layer. The PDU generator forwards the PDUs to the allocation procedure unit in the data link layer, which allocates the PDUs to MEO and GEO paths based on a pattern indicated by the allocation algorithm running in the Unified Software Defined Radio Controller (uSRC). The uSRC is connected to GSJNC over control plane logical link to exchange signalling and optimization information between the UT and the HGS. Whilst the PDU allocation is ongoing at the data link layer of the UT, the PDUs are encapsulated to Generic Stream Encapsulation (GSE) by the encapsulator and then forwarded for base-band framing; subsequently, the Base-band Frames (BBFrame) are transmitted over the satellite channel. At the HGS receiver, they are decapsulated into GSE packets and then reconstructed to PDUs in the data link layer on the MEO and GEO paths. The PDUs from both paths are then aggregated by the traffic merger at the network layer. The following procedure is the PDU integrity check and ordering that are performed with intelligence provided by the GSJNC, which has knowledge of the PDU original order.

The conditions for the hybrid allocation algorithm to be implemented includes:

1) The MEO and GEO satellites must have visibility to the HGS and the UT.
2) The link budget must be satisfied for both MEO and GEO with adequate link margin.
3) Network connectivity requirement in the service level agreement (SLA) must be for at least 24 hours and above.
4) The UT must support DC functionality.

B. Satellite Link and Channel Model

The satellite is designed with a link budget and air interface that has the capability of mitigating fading in a communication channel, by employing modulation and coding schemes to

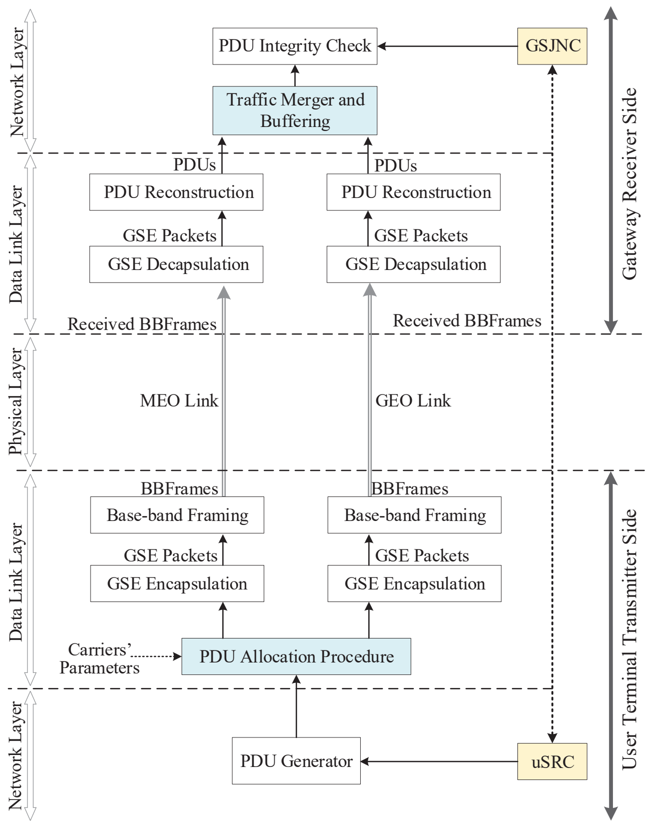

Fig. 2. System Architecture

adapt to the signal-to-noise ratio of the channel. From the Friis equation as described in [12], the received power which is measured in dB, is composed of the summation of the transmitted power (P_T), gain of transmitting antenna (G_T), gain of receiving antenna (G_R) and the deductions comprising the free space loss (FSL), atmospheric absorption and other propagation loses. The FSL is presented below in (1).

$$FSL = 20\log(\frac{4\pi D}{\lambda}) \quad (1)$$

Where D is the propagation distance in meters and λ is the wavelength of the radio frequency also in unit of meters. The SNR at the receiver is obtained to understand the total power degradation in dB. The channel noise is impacted by the assigned channel bandwidth in addition to the antenna thermal noise and other losses. To estimate the communication signal quality and taking into consideration the Friis equation earlier discussed, the energy-per-bit-to-noise ratio (E_b/N_o) which is also SNR normalized to spectral efficiency, is expressed in (2).

$$E_b/N_o = EIRP + G_R - FSL - L_{oth} - N_o - 10\log(R_B) \quad (2)$$

Where EIRP represents computation of Effective Isotropic Radiated Power which comprises of P_T, and G_T, while L_{oth}, N_o and R_B represent other losses, noise spectral density and bit rate respectively [12]. The impairments in the channel greatly affects the demodulated data at the receiver, and this is seen in the increase of the E_b/N_o required to achieve a given bit error rate (BER), typically considered around 10^{-6}. The E_b/N_o required to close the link budget with a good margin, is obtained from the air interface which comprises of combinations of modulation and coding schemes.

C. Problem Analysis

The problem of uplink delay and capacity can be solved by utilizing the two channel paths of GEO and MEO to simultaneously transmit the PDUs from the UT to the HGS. The Poisson arrival process is assumed at the HGS with PDU inter-arrival times of λ_M and λ_G for MEO and GEO respectively. The PDUs that arrive at the HGS through the MEO link were initially transmitted with a probability of P_M, while those over the GEO link were transmitted with a probability of P_G. Hence the corresponding PDU inter-arrival time over the MEO and GEO links is represented as $P_M\lambda_M$ and $P_G\lambda_G$ respectively. The average delay of the hybrid PDUs at HGS is expressed as stated in (3) below [13], with d_{G_i} and d_{M_i} representing delay on the GEO and MEO links respectively, for the i^{th} block of PDUs.

$$\mathbb{E}[d] = \sum_{i=1}^{n} P_{G_i} d_{G_i} + \sum_{i=1}^{n} P_{M_i} d_{M_i} \quad (3)$$

The GEO delay can be computed while considering a PDU processing time at the UT and HGS as β_G; similarly β_M is considered as the PDU processing time for MEO. The delay of MEO PDU is expressed as

$$d_{M_i} = \lambda_{M_i} + \beta_{M_i} \quad (4)$$

Similarly the delay on the GEO PDU can be given as

$$d_{G_i} = \lambda_{G_i} + \beta_{G_i} \quad (5)$$

The probability that a PDU will arrive through the GEO channel can be expressed as

$$P_{G_i} = \frac{\lambda_{M_i}}{\lambda_{G_i}} \quad (6)$$

Furthermore, the probability that a PDU will arrive through the MEO channel is

$$P_{M_i} = 1 - P_{G_i} = 1 - \frac{\lambda_{M_i}}{\lambda_{G_i}} \quad (7)$$

Substituting (4), (5), (6) and (7) into (3) will result in the average PDU delay

$$\mathbb{E}[d] = \sum_{i=1}^{n} [\frac{\lambda_{M_i}}{\lambda_{G_i}}[\lambda_{G_i} + \beta_{G_i}] + (1 - \frac{\lambda_{M_i}}{\lambda_{G_i}})[\lambda_{M_i} + \beta_{M_i}]] \quad (8)$$

Subject to:

$$\mathbb{C}_1 : 0 < \lambda_{M_i} < \lambda_{G_i} \;\; \forall i \in N, i = 1, ..., n$$

$$\mathbb{C}_2 : min(\lambda_{G_i}, \lambda_{M_i}) < \infty \;\; \forall i \in N, i = 1, ..., n$$

$$\mathbb{C}_3 : P_{G_i} = \frac{\lambda_{M_i}}{\lambda_{G_i}} > 0 \;\; \forall i \in N, i = 1, ..., n$$

$$\mathbb{C}_4 : P_{M_i} = 1 - \frac{\lambda_{M_i}}{\lambda_{G_i}} > 0 \ \forall i \in N, i = 1, ..., n$$

Following appropriate scheduling of the PDUs on the two channel paths at the UT, the MEO and GEO PDUs that arrive the HGS at the same time will be aggregated at the traffic merger, thereby optimizing throughput by increasing the bandwidths. Throughput at HGS can be expressed using the Shannon capacity for a noisy channel. The SNR will be obtained from the link budget, and then the combined capacity of the hybrid system for both MEO and GEO bandwidths can be expressed as an aggregated capacity (H_C). Here B_G, B_M, SNR_G and SNR_M are the GEO bandwidth (in MHz), MEO bandwidth (in MHz), GEO link SNR (dB) and MEO link SNR (dB) respectively.

$$\begin{aligned} H_C(Mbps) \ = \ & \sum_{i=1}^{n} P_{G_i}[B_G \log_2(1 + SNR_{G_i})]) \\ & + \sum_{i=1}^{n} P_{M_i}[B_M \log_2(1 + SNR_{M_i})] \end{aligned} \quad (9)$$

Subject to C_1, C_2, C_3, C_4 and C_5 for DC.

$$\mathbb{C}_5 : SNR_{M_i} \geq SNR_{G_i} \quad \forall i \in N, i = 1, ..., n,$$

D. Proposed Resource Allocation Algorithm

The hybrid resource allocation (HRA) algorithm is proposed in Algorithm 1 to optimize the GEO delay and throughput by activating DC with the addition of a MEO link that has a limited visibility period due to the lower altitude. As discussed earlier, the GSNJC collects the signalling measurements of the MEO and GEO links, it evaluates if the conditions for DC are met and then instructs the uSRC to implement the uplink DC optimization with a defined pattern of the resource allocation in the hybrid algorithm 1. The objective of the algorithm is to connect the fixed UT to MEO and GEO links for uplink transmission and the algorithm is periodically executed to take into consideration the current values of the input variables. The inputs to the algorithm include PDU inter-arrival time, Doppler shift and SNR for intelligent decision making. The first phase of the algorithm is to generate the carrier allocation sequence for both GEO and MEO using (6) and (7) respectively. Once the allocation sequence is obtained, the vectors C_1 and C_2 are combined and saved as M, which allows for the aggregation of the PDUs over the dual connected links. The next phase in the algorithm is the decision process for the carrier allocation implementation; this phase utilizes the inputs mentioned earlier to effect the implementation decision. The algorithm considers the three variables to make a cascaded decision flow. If the MEO PDU inter-arrival time is less than that of GEO, and if the MEO SNR and Doppler shift are greater or equal to that of GEO, the decision is to implement DC with the M allocation sequence, else the algorithm will revert to a single carrier mode on C_1 (GEO).

Algorithm 1: Hybrid Resource Allocation

Input: λ_M = MEO PDU Inter-arrival Time
λ_G = GEO PDU Inter-arrival Time
α = Total blocks of PDUs
D_M = MEO Doppler Shift
D_G = GEO Doppler Shift
SNR_G = GEO SNR
SNR_M = MEO SNR
$i = 1$

while $i \leq \alpha$ **do**
  Generate Carrier Allocation Sequence
  For GEO Carrier
  $C_1 = \frac{\lambda_{M_i}}{\lambda_{G_i}}$ from (6)
  For MEO Carrier
  $C_2 = (1 - \frac{\lambda_{M_i}}{\lambda_{G_i}})$ from (7)
  Combine both vectors and store Carrier Allocation Sequence in M
  $M = [C_1, C_2]$
  Implement Carrier Allocation
  if $\lambda_M < \lambda_G$ **then**
    if $SNR_M \geq SNR_G$ **then**
      if $D_M \geq D_G$ **then**
        Implement DC with M = $[C_1, C_2]$
      else
        Activate Single Carrier mode on C_1
      end
    else
      Activate Single Carrier mode on C_1
    end
  else
    Activate Single Carrier mode on C_1
  end
end

III. Performance Evaluation

In this section, the simulation system is setup with defined parameters. The simulation results are also discussed to evaluate the performance of the system architecture and the proposed hybrid allocation algorithm.

A. System Simulation Setup

In Table I, the link budget and parameters are shown for both MEO and GEO links, DVBS2X is used as the air interface. The GEO satellite is set at an altitude of 35,786 km, while MEO was simulated to operate at 8,000 km from the earth surface using STK 12.4. The results of the Eb/No in dB from the link budget can be seen in Fig 3. It is observed that MEO has 12 instances of link closure (with assumed 8 hours total link visibility time in a 24 hours period), while GEO has a steady link closure trend for a period of 24 hours. Based on the uniqueness of the MEO channel, which has a lower altitude from the earth surface compared to GEO, the satellite moves away and returns to the UT location with different Doppler shift values. Hence the Doppler shift of the satellite in KHz is shown in Fig 4. Furthermore in Fig. 5, the PDU inter-arrival time for MEO and GEO is derived from the propagation delay of the STK simulation, it can be seen that MEO varies between 0.005s to 0.016s, while GEO is between 0.98s to 0.117s. Hence the (approximate) average PDU inter-arrival time for MEO and GEO is further obtained as 11ms and 108ms respectively.

TABLE I
LINK PARAMETERS

Parameters	MEO	GEO
Satellite Altitude (Km)	8,000	35,786
UT Latitude (Degrees)	11.92	11.92
UT Longitude (Degrees)	77.69	77.69
Gateway Latitude (Degrees)	1.44	1.44
Gateway Longitude (Degrees)	38.43	38.43
Flux Density (dBW/m^2)	-106.86	-120.77
Carrier Frequency (GHz)	14	14
Waveform	DVBS2X	DVBS2X
Free Space Loss (dB)	184	205
Carrier Bandwidth (MHz)	50	50
EIRP (dBW)	33.73	39.73

B. System Performance Evaluation

In Fig. 6, the delay of the HRA is evaluated with comparison to the round robin (RR) scheduler, a load-balancing (LB) scheduler in [14] and the single GEO carrier. The delay result in ms is plotted against the number of transmitted PDUs. The HRA was implemented by defining the parameters in (8), including parameters like PDU inter-arrival time which was obtained from the average of the inter-arrival time of MEO (11 ms) and that of GEO (108 ms) as explained in subsection III-A. Likewise the probability to transmit over either MEO or GEO was formulated as in (7) and (8) then inserted into the algorithm. The probability is a function of the inter-arrival time and for this simulation, P_G was 1/9 and P_M was 8/9; this indicates that during any transmission instance, 8 out of 9 PDUs will be transmitted over the MEO channel while the remaining PDU will be transmitted over the GEO channel using the HRA. The RR scheduler utilizes the PDU transmission allocation weighting of 50% PDUs transmitted over MEO and the remaining 50% will be sent over the GEO channel. For load-balancing scheduler, it allocates PDUs on a weighting factor of 67% on the carrier with the best SNR, and in this model that will be the MEO carrier, while the remaining 33% on the GEO carrier. In HRA, the weighting is defined so that 89% of the PDUs are transmitted using MEO and the remaining 11% over the GEO channel. By so doing, the algorithm leverages the lower delay on MEO over GEO to achieve a better performance compared to RR and LB. The result of transmitting 10,000 PDUs is that the delay on the single GEO carrier, RR and LB are 1,079 ms, 594 ms and 432 ms respectively, while the HRA yields a delay of 208 ms as shown in Fig. 6. This shows HRA has a delay performance gain that is 70%, 96% and 135% less than LB, RR and single GEO carrier respectively.

The peak data rate was obtained for the GEO and the aggregated carriers using (9). The carrier bandwidth used for

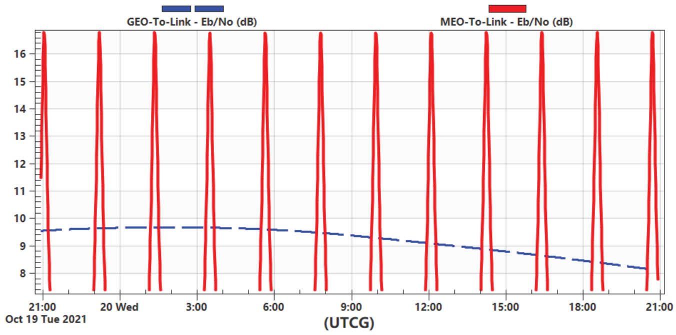

Fig. 3. A comparison between Eb/No of MEO and GEO Links verses Time.

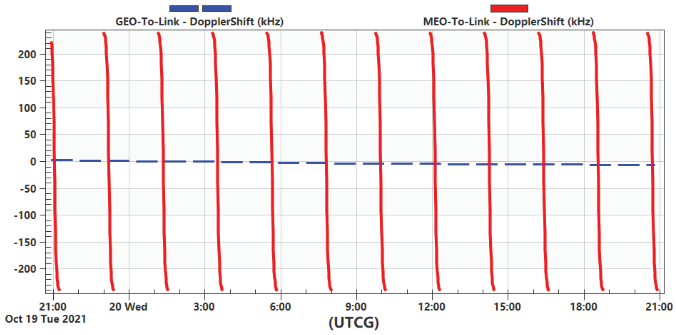

Fig. 4. A comparison between Doppler Shift of MEO and GEO Links verses Time.

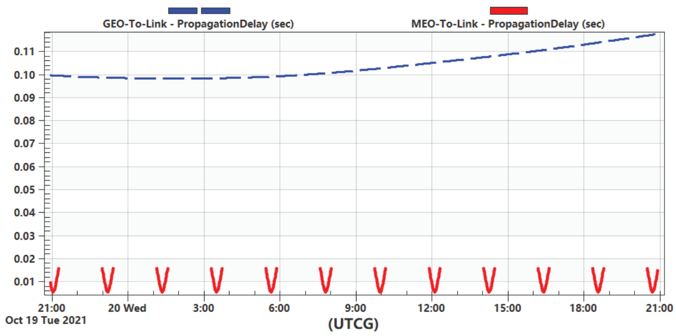

Fig. 5. A comparison between PDU Inter-arrival Time (delay) of MEO and GEO Links verses Time.

both MEO and GEO was 50MHz, and the SNR was obtained from the link Eb/No simulations in subsection III-A. In Fig. 7, the peak data rate is plotted against SNR, and it is observed that the achievable peak data rate for the RR, LB and HRA are 155 Mbps, 168 Mbps and 186 Mbps respectively. Again HRA shows an improvement of approximately 18% and 10% over RR and LB scheduler respectively. However at very low SNR values, LB and RR have better throughput performance than HRA.

In Fig. 8, the achievable peak data rate is evaluated for the various schedulers and algorithms while increasing the bandwidth of the MEO carrier to a maximum of 120 MHz. The result obtained shows the RR, LB and HRA yielded 292 Mbps, 351 Mbps and 429 Mbps respectively in peak data rate. This reveals that HRA out performs RR and LB schedulers by 38% and 20% respectively; hence it is more superior in achieving higher KPI values.

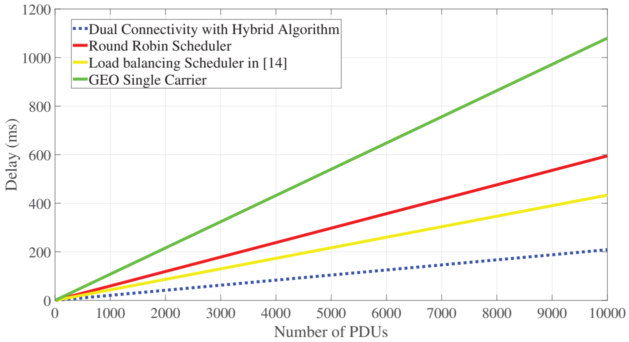

Fig. 6. Delay verses number of PDUs.

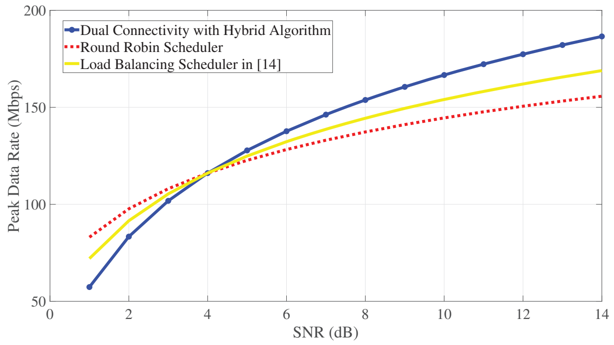

Fig. 7. Uplink peak data rate verses SNR.

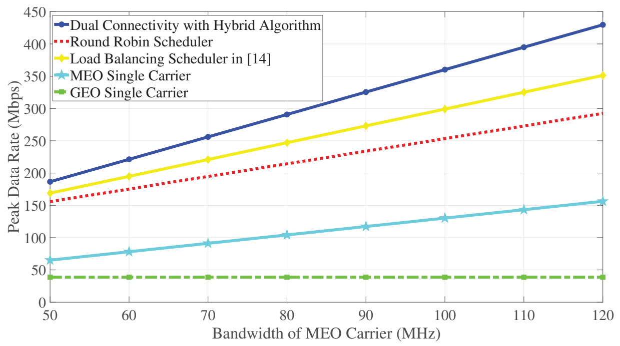

Fig. 8. Uplink peak data rate verses MEO carrier bandwidth.

IV. Conclusions

In this paper, the uplink throughput and delay of a satellite network is optimized using DC technique and aggregating the two carriers involved. A network architecture was designed for a multi-orbital satellite system, where the diversity gains of CA was employed at higher layers, with a software defined network controller at the network layer performing dynamic resource allocation. The hybrid resource allocation algorithm operates at the controller performing optimum dynamic flow control and traffic steering by considering the availability of resources and the channel propagation information of the orbital links to define the resource allocation pattern in enhancing uplink system performance. The designed hybrid resource allocation algorithm outperformed the single GEO carrier, traditional RR scheduler and the LB scheduler by 135%, 96% and 70% respectively in the average delay performance. Similarly, the peak data rate achieved on the HRA showed improvements of 18% and 10% above RR and LB respectively, when both MEO and GEO carriers are configured with same bandwidth of 50 MHz. Even when the MEO carrier bandwidth was increased to 120 MHz, the HRA outperformed both RR and LB by 38% and 20% respectively. In addition, the proposed multi-orbital architecture showed through simulations improvement over a single GEO satellite network in delay and throughput KPIs.

A future research component that can be explored includes evaluating different service types with varying QoS requirements that is designed in a network slicing architecture with traffic routing algorithms to meet the dynamic service requirement. Another future research area is the design of an energy efficient scheduler, that will ensure energy conservation for the UT.

Acknowledgement

This work is financially supported by Fond National de la Recherche (FNR), under the Industrial Partnership Block Grant (IPBG) ref 14016225, project known as INSTRUCT: INtegrated Satellite – TeRrestrial Systems for Ubiquitous Beyond 5G CommunicaTions Networks. The views of the authors do not necessarily reflect the views of FNR.

References

[1] M. A. Lema, E. Pardo, O. Galinina, S. Andreev, and M. Dohler, "Flexible dual-connectivity spectrum aggregation for decoupled uplink and downlink access in 5G heterogeneous systems," *IEEE J. Sel. Areas Commun.*, vol. 34, no. 11, pp. 2851–2865, 2016.

[2] C. Pupiales, D. Laselva, and I. Demirkol, "Capacity and congestion aware flow control mechanism for efficient traffic aggregation in multi-radio dual connectivity," *IEEE Access*, vol. 9, pp. 114 929–114 944, 2021.

[3] 3rd Generation Partnership Project (3GPP), "Study on small cell enhancements for E-UTRA and E-UTRAN: Higher layer aspects," Standard, 2014.

[4] G. S. Park and H. Song, "Video quality-aware traffic offloading system for video streaming services over 5G networks with dual connectivity," *IEEE Trans. Veh. Technol.*, vol. 68, no. 6, pp. 5928–5943, 2019.

[5] H. Al-Hraishawi, N. Maturo, E. Lagunas, and S. Chatzinotas, "Scheduling design and performance analysis of carrier aggregation in satellite communication systems," *IEEE Trans. Veh. Technol.*, pp. 1–14, 2021.

[6] J. Du, C. Jiang, H. Zhang, Y. Ren, and M. Guizani, "Auction design and analysis for SDN-based traffic offloading in hybrid satellite-terrestrial networks," *IEEE J. Sel. Areas Commun.*, vol. 36, no. 10, pp. 2202–2217, Oct. 2018.

[7] A. J. Roumeliotis, C. I. Kourogiorgas, and A. D. Panagopoulos, "Optimal dynamic capacity allocation for high throughput satellite communications systems," *IEEE Wireless Commun. Lett.*, vol. 8, no. 2, pp. 596–599, Apr. 2019.

[8] M. G. Kibria, E. Lagunas, N. Maturo, H. Al-Hraishawi, and S. Chatzinotas, "Carrier aggregation in satellite communications: Impact and performance study," *IEEE Open J. Commun. Soc.*, pp. 1390–1402, 2020.

[9] ETSI TR 102 376-2, "Digital Video Broadcasting (DVB): Implementation guidelines for the second generation system for broadcasting, interactive services, news gathering and other broadband satellite applications;part 2: S2 extensions (DVB-S2X)." European Telecommunications Standards Institute, Standard, 2015, (http://www.etsi.org).

[10] O. N. C. Yilmaz, O. Teyeb, and A. Orsino, "Overview of LTE-NR dual connectivity," *IEEE Commun. Mag.*, vol. 57, no. 6, pp. 138–144, 2019.

[11] B. Elbert, *The Satellite Communication Ground Segment and Earth Station Handbook*, 2nd ed. Artech House, 2014.

[12] A. Al-Saegh, A. Sali, J. Mandeep, A. Ismail, A. Al-Jumaily, and C. Gomes, *Atmospheric Propagation Model for Satellite Communications*. IntechOpen, 2014, ch. 09, p. 28.

[13] V. Ramaswamy, J. T. Correia, and D. Swain-Walsh, "Modeling and analysis of multi-rat dual connectivity operations in 5g networks," in *2019 IEEE 2nd 5G World Forum (5GWF)*, 2019, pp. 484–489.

[14] H. Al-Hraishawi, N. Maturo, E. Lagunas, and S. Chatzinotas, "Perceptive packet scheduling for carrier aggregation in satellite communication systems," *IEEE Int. Conf on Commun. (ICC)*, pp. 1–6, Jun. 2020.